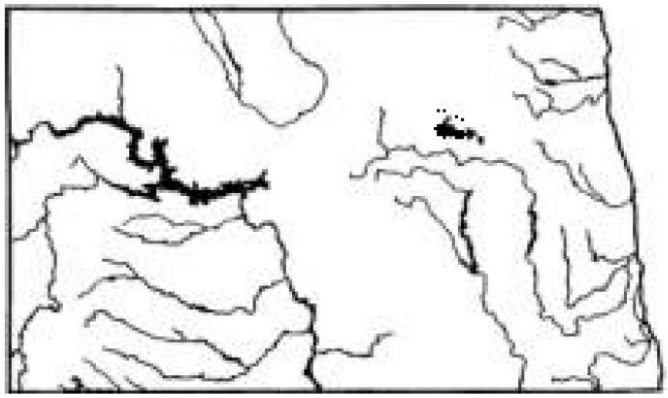

Technical Report No: ND12-06

Development of Fe-GAC Adsorbent for Arsenic Removal

Qigang Chang
Environmental and Conservation Science Graduate Program

Wei Lin
Dept. of Civil Engineering
North Dakota State University
Fargo, North Dakota

June 2012

North Dakota Water Resources Research Institute
North Dakota State University, Fargo, North Dakota

Technical Report No: ND12-06

Development of Fe-GAC Adsorbent for Arsenic Removal

Qigang Chang
WRRI Graduate Research Fellow
Environmental and Conservation Sciences Graduate Program

Wei Lin
Associate Professor, Department of Civil Engineering
North Dakota State University

June 2012

The work upon which this report is based was supported in part by federal funds provided by the United States of Department of Interior in the form of ND WRRI Graduate Research Fellowship for the graduate student through the North Dakota Water Resources Research Institute.

Project Period: March 1, 2008 - February 28, 2011
Project Number: 2008ND168B and 2009ND186B

North Dakota Water Resources Research Institute
Director: G. Padmanabhan
North Dakota State University
Fargo, North Dakota 58108

TABLE OF CONTENTS

LIST OF TABLES

LIST OF FIGURES

ACKNOWLEDGMENTS

Stipend support and supplemental funding from the North Dakota Water Resources Research Institute (ND WRRI) are thankfully acknowledged.

ABSTRACT

Granular activated carbon (GAC) was impregnated with iron through a new multi-step procedure using ferrous chloride as the precursor for removing arsenic from drinking water. Scanning electron microscopy (SEM) and energy dispersive X-ray spectroscopy (EDS) analysis demonstrated that the impregnated iron was distributed evenly on the internal surface of the GAC. Impregnated iron formed nano-size particles, and existed in both crystalline (akaganeite) and amorphous iron forms. Iron-impregnated GACs (Fe-GACs) were treated with sodium hydroxide to stabilize iron in GAC and impregnated iron was found very stable at the common pH range in water treatments. The impact of the amount of impregnated iron in granular activated carbon (GAC) on arsenic adsorption capacity and kinetics was investigated at an arsenic concentration range that is typical for drinking water in this study. Results showed that the iron content of Fe-GAC reduces the arsenic adsorption rate and a five days adsorption time is necessary in the isotherm tests. The initial arsenic adsorption rate decreased with more impregnated iron, which is probably caused by the reduced pore size of Fe-GACs that is confirmed in the BET analysis. Langmuir model regression through a new approach disclosed that the amounts of impregnated iron affect arsenic adsorption capacity significantly. The maximum adsorption capacity (q_m) increased greatly with the iron content for both As(V) and As(III). When iron content is higher than 13.59%, more iron contributes less to arsenic adsorption capacity or even exhibits negative impact. Interestedly, the iron content has no impact on arsenic adsorption affinity. The adsorption affinity of Fe-GAC is 0.0223 L/μg for As(V) and 0.0170 L/μg for As(III). The specific surface area of impregnated iron was estimated according to the BET instrumental analysis of Fe-GACs. The surface area of impregnated iron shows the same trend as the arsenic adsorption capacity obtained in isotherm tests. At the iron content of 13.59%, impregnated iron possesses the highest specific surface area of 473 m^2/g. Column tests showed that Fe-GACs can remove arsenic below the maximum contaminant level (10 μg/L) of arsenic in drinking water. The performance of Fe-GAC at breakthrough (10 μg/L) was enhanced significantly with increase of the amounts of impregnated iron. The number of bed volume (BV) treated at breakthrough increased from 140 to 1000 when the iron content of Fe-GACs increased from 4.56% to 13.59%. With further increase of iron content from 13.59% to 28.90%, BV treated at breakthrough slightly reduced from 1000 to 850. The utilization rate of Fe-GACs at breakthrough varied between 18.2% and 35.6%. The slope of breakthrough curves became smaller with increase of iron content, which implies that arsenic intraparticle diffusion rate in Fe-GACs decreased with iron content. Longer EBCT is required to achieve better use of Fe-GAC with high iron contents due to slow arsenic intraparticle diffusion.

INTRODUCTION

Arsenic is a ubiquitous element in the environment and can be found in rocks, waters, and soils. It enters drinking water supplies from natural deposits in the earth as well as from anthropogenic activities, such as agricultural and industrial practices (*1*). Arsenic can cause serious health problems, such as cancers of bladder, lung, skin, kidney, liver, and prostate (*2, 3*). The USEPA has enforced a new arsenic standard for drinking water of 10 µg/L to protect people from the effects of long-term chronic exposure to arsenic since 2006 (*4*).

Iron impregnated granular activated carbon (Fe-GAC) can remove arsenic from the aqueous phase effectively (*5-12*). Impregnation eliminates the disadvantages of using iron-based materials alone, such as poor mechanic strength, small specific surface area, and requirement for follow up filtration (*6, 12*). The primary advantage of GAC as the impregnation support is its huge internal surface area and advanced pore structure (*13*). When iron is evenly distributed inside GAC, the huge internal surface area of GAC can be largely used for iron impregnation and impregnated iron exhibits great adsorption capacity (*11, 12*).

Since impregnated iron is recognized the active phase that enhances arsenic adsorption capacity of GAC, more iron was preferred in iron impregnation (*5, 8*). However, several studies showed that arsenic adsorption capacity did not increase proportionally to the increase of iron at high iron content (*6, 12, 14*). The percentage of arsenic adsorption was found to decrease with iron content when iron content was above 6% (*6*). Chang et al. (*12*) conducted a further study and used a more direct indicator, arsenic adsorption capacity, to demonstrate the relationship between iron content and adsorption capacity. They found that the maximum arsenic adsorption capacity was reached at the iron content of 4.22% and the iron impregnation method also affects the iron content that shows the maximum arsenic adsorption capacity. Even though both BET surface area and pore volume were reported to decrease with iron impregnation (*6, 15-17*), a direct link between arsenic adsorption capacity and BET surface/Pore structure of Fe-GAC is still missing. It is still a speculation that the reduction of total surface area and blockage of pores caused arsenic adsorption capacity to reduce at high iron content. Further research is needed to systematically investigate how iron content affects the arsenic adsorption capacity.

Adsorption kinetics is as important as adsorption capacity because it depicts the uptake rate of adsorbate and controls the equilibrium time of the adsorption process (18, 19). A few studies investigated arsenic adsorption kinetics on iron impregnated activated carbon and different kinetic models, including parabolic diffusion model, pseudo-first-order model, and pseudo-second order model, were used to interpret the arsenic adsorption (8, 17, 20). Because impregnated iron changes the GAC pore structure, it most likely will affect arsenic diffusion rate. Although a number of kinetic studies have investigated arsenic adsorption on Fe-GAC, little information is available on the effect of the amount of impregnated iron on arsenic adsorption kinetics. The objectives of this study were to: (1) develop a method to impregnate GAC with a high amount of iron that is stably and evenly distributed in GAC; (2) characterize Fe-GAC to determine the amount, distribution, morphology, and species of impregnated iron; (3) investigate impacts of the amount of impregnated iron on arsenic adsorption capacity and efficiency; (4) As (III) and As(V) adsorption characteristics of Fe-GACs with different iron contents at a low arsenic concentration range; and (5) the impact of iron content on the pore structure and surface area of Fe-GACs.

MATERIALS AND METHODS

Materials

Lignite-based GAC Darco 20×50 (American Norit Co. Inc) was thoroughly washed using de-ionized (DI) water to clean impurities and powder, dried at 105°C overnight, and stored in desiccators for iron impregnation.

Standardized As(III) ($NaAsO_2$) 0.1N solution (Alfa Aesar Co.) was used for preparation of As(III) solution. Sodium arsenate (Na_2HAsO_4) was used for preparation of As(V) solution. Ultra Scientific certified standard As(V) solution (1000 mg/L in 2% nitric acid) was used for preparation of calibration standards in arsenic instrumental analysis. All other chemicals used in this study were of reagent grade and used as received, including ferrous chloride, sodium arsenate, hydrochloric acid, nitric acid, sodium hydroxide, and sodium bicarbonate.

Groundwater samples were taken from a farmer's well at the former arsenic trioxide Superfund site (Site ID #0800522) near the City of Wyndmere, North Dakota (*21*). DO, temperature, specific conductivity, and pH were measured on-site; other parameters, total phosphate, TOC, turbidity, and arsenic, were determined in laboratory. Groundwater samples were stored at 4°C.

Preparation of Fe-GAC

The multi-step iron impregnation procedure developed by Chang et al. (*12*) was modified in this study by the addition of a stabilization step using sodium hydroxide. This sodium hydroxide post-treatment converts impregnated iron to ferric hydroxide which was identified later as akaganeite in X-Ray Diffraction (XRD) analysis. This stabilization step improves iron impregnation efficiency by reducing the lost of impregnated iron in the impregnation process, enhances the stability of impregnated iron, and increases arsenic adsorption capacity by generation of favored iron species - hydrous ferric hydroxide that has poor crystalline structure and large surface areas (*22*). The modified iron impregnation procedure is: (1) GAC reacts with ferrous chloride solution on a rotating shaker for 24 hr; (2) GAC particles are separated, and dried in a convective oven for 10 hr; (3) Fe-GAC is treated with 1 N NaOH solution for 10 hr; and (4) Fe-GAC is washed with DI water. The above process is repeated to produce Fe-GACs with desired iron amount. In this study, Fe-GACs have been prepared with 11 different iron contents ranging from 4.56% to 28.90%. SEM analyses indicated that iron impregnated through this method is evenly distributed inside GAC.

Characterization of Fe-GAC

Fe-GACs were evaluated based on four indicators: amount of impregnated iron, distribution of impregnated iron, stability of impregnated iron, and arsenate adsorption capacity of Fe-GAC. Iron content (defined in (Eq. (1)) was determined through an acid extraction method. Distribution and morphology of impregnated iron were measured by scanning electron microscopy (SEM) and energy dispersive X-ray spectroscopy (EDS). Iron species were identified by X-ray diffraction (XRD). According to the objectives of this study, the pore structure and surface chemistry of Fe-GACs were not investigated.

$$Iron\ content = \frac{mass\ of\ iron}{mass\ of\ GAC + mass\ of\ iron} \times 100\% \qquad (1)$$

Measurement of iron content

Three different methods, incineration (*23*), incineration and digestion (*8*), and acid extraction (*24*), were evaluated for the measurement of the amount of impregnated iron in GAC (Appendix III). The acid extraction method was selected and modified for this study. Three hundred milligrams of Fe-GAC was added into a 40-mL vial containing 30 mL 1:1 HCl solution and shaken for 10 h. Then, the vial was placed in a water bath at 70-80 °C for 4 h. The Fe-GAC was separated from the solution using GF/C filter paper. The iron concentration in the filtrate was analyzed using the phenanthroline method with a Hach spectrophotometer DR5000.

Measurement of the distribution, morphology, and species of impregnated iron

Fe-GACs were fractured to expose the internal structure for the examination of the distribution and morphology of impregnated iron using a JEOL JSM-6490LV scanning electron microscope equipped with a Thermo Energy Dispersive X-ray System. To avoid the destruction of the surface characteristics of Fe-GACs, no further polishing action was conducted on exposed cross-sections.

XRD analysis was carried out to determine iron species in GACs using a Bruker AXS' D8 Discover diffractometer in Bragg-Brentano geometry, using Cu Kα radiation with a wavelength of 1.5406 nm. The powdered samples of Fe-GACs were scanned from 5° to 85°, using a step size of 0.02° and a run time of 1 sec/step.

Iron Desorption Test

This test was conducted to evaluate the stability of impregnated iron. Five hundred milligrams of Fe-GAC was added to 40 mL DI-water and shaken 48 h. Fe-GACs were separated through filtration using GF/C filter paper. The iron concentration in the filtrate was analyzed using the same method described in Section 3.2.3.1. Desorption of impregnated iron was evaluated according to the mass of dissolved iron in DI-water.

Adsorption Kinetic Test

One hundred milligrams of Fe-GAC were added into a number of 40-mL vials containing 35 mL 3mg/L As(V) solution with pH controlled at 7.0 using a 0.05N $NaHCO_3$ buffer solution. The bicarbonate buffer solution was found to have no impact on arsenic adsorption using iron based materials (*25, 26*). These vials were placed on the rotating shaker at 30 rpm and 25°C. A vial was taken from the shaker to determine the arsenic concentration in the aqueous phase. The filtration process used 0.45 µm membrane filter papers. Adsorption kinetic tests were carried out for Fe-GAC with iron contents of 5.57-28.90%.

Adsorption Isotherm Test

The arsenic adsorption capacities of Fe-GACs were evaluated in batch experiments. One hundred milligrams of Fe-GAC was added into 40-mL vials containing 35 mL arsenic solutions. The initial concentrations of the arsenic solution for isotherm tests varied between 200 µg/L and 3000 µg/L, which was to achieve the desired arsenic equilibrium concentration of < 250 µg/L to simulate the range of typical water treatment. To prevent the oxidation of As(III), nitrogen purged DI-water was used in preparation of As(III) solutions. The pH of adsorption tests was controlled at 7.0 using a 0.05 N $NaHCO_3$ buffer solution. After 5 days of shaking at 30 rpm and 25°C, Fe-GACs were separated from the solution using 0.45 µm membrane filter papers. The

filtrate was preserved by 6 N HNO_3 and stored at 4°C for arsenic analysis. The same procedure was used for the adsorption isotherm tests on groundwater samples.

Fe-GAC Surface Area and Pore Volume Measurement

The liquid nitrogen adsorption-desorption isotherms of Fe-GACs with different iron contents at 77 K were measured using Micro-meritics ASAP 2020 to characterize the surface area and the porous structure of Fe-GACs. Prior to measurement, Fe-GACs were degassed at 105°C under nitrogen flow for 12 hr. BET model was used for the calculation of surface area of Fe-GACs.

Column Test

Borosilicate glass columns with an inner diameter of 7 mm were used in breakthrough tests. The mean size of Fe-GAC is 0.5 mm so that the ratio of diameter of column to particle size of adsorbent is around 14, which is smaller than commonly recommended value of 20 to avoid "channeling" (*19*). Because the main objective of column tests in this study is to evaluate the impact of iron content of Fe-GACs on arsenic breakthrough rather than a pure design purpose, the small size of column is acceptable. In addition, special measures were taken to minimize "channeling". Fe-GACs were soaked in DI-water for 48 hours to degas prior to addition to columns. To avoid entrainment of air during column preparation, wetted Fe-GAC was transferred to columns filled with de-ionized (DI) water. DI-water was used for initialization of Fe-GAC packed column for flow-rate adjustment and compaction of Fe-GAC bed. Then, influent was switched to groundwater to start tests. At two ends of Fe-GAC bed, glass wool was added to avoid loss of Fe-GACs during tests. All tubes used were Tygon tubing and fittings were HDPE or PVC to minimize the possible arsenic adsorption. Arsenic solution was continuously fed into the column using a Cole-Parmer Master peristaltic pump in an up-flow pattern to minimize "channeling" as well. In the full-scale column parallel tests, it was found that EBCTs of 6.3 min and 3 min with granular ferric hydroxides (GFH) resulted in nearly identical arsenic breakthrough curves. Samples were collected from the sampling port at the up-end of column at predetermined time and filtered through 0.45 membrane syringe filter. Filtrate was saved at 4 °C for arsenic analysis. The flow-rate was monitored daily.

Analytical Methods

Arsenic concentration in water samples was determined using a Perkin Elmer 4110ZL Graphite Furnace Atomic Absorption Spectrometer (GFAAS) at 193.7 nm in accordance with the EPA method 200.9 Rev.3.0 (*27*). A calibration curve with arsenic concentrations of 0, 2, 5, 15, 30, and 60 µg/L was prepared using an As(V) standard solution (1000 µg/mL in 2% nitric acid, Ultra Scientific certified). A linear response with correlation coefficient (R^2) higher than 0.999 was achieved. This method had an arsenic detection limit of 1 µg/L. For the analytical quality control, an instrument performance check (IPC) solution (30 µg/L) and calibration blank were analyzed after every 10 samples. The GFAAS was programmed to recalibrate the arsenic analytical method if a 10% variation of IPC was observed. Additionally, spiked experimental blanks/samples were adopted as quality control measures and the recovery rate was 95-105%. The iron concentration was analyzed through the phenanthroline method with a Hach spectrophotometer DR5000.

RESULTS AND DISCUSSION

Preparation of Fe-GAC

It is difficult to achieve high amounts, even distribution, and stability for impregnated iron inside GAC in one step. This new synthesizing method is a multi-step procedure in which a small amount of iron is impregnated in GAC to achieve full penetration and even distribution in each step. Then, by repeating this process, high amounts of iron can be achieved as well as an even iron distribution inside GAC. Ferrous was used as the precursor because it is soluble at a wide range of pH and can diffuse deep into the internal pores of GAC (*6*). However, ferrous impregnated in GAC may not be stable because it can re-dissolve into solution. Therefore, in the synthesis process, the drying step was purposely extended to 10 h to stabilize iron inside GAC by the conversion of ferrous to ferric using oxygen in air in the convective oven. In this step, most ferrous chloride is expected to be oxidized to ferric chloride, ferric oxide, and ferric hydroxide.

Two GACs, Darco 20×50 and Norit RX3 EXTRA, were used for iron impregnation to examine the capability of this synthesizing method. As shown in Figure 1, iron contents were 2.03% for Darco 20×50 and 0.77% for Norit RX3 EXTRA after the first 24 h treatment. Iron contents increased almost linearly with repetitions, 1.03% per repetition for Darco 20×50 and 0.74% per repetition for Norit RX3 EXTRA. If all pores of GAC are assumed to be filled with 0.5 M ferrous solution ideally in each repetition, according to the total pore volumes of GACs, the impregnated iron is 26.6 mg/g for Darco 20×50 and 19.4 mg/g for Norit RX3 EXTRA per repetition. Therefore, the ideal increment of iron content in each repetition will be 2.60% for Darco 20×50 and 1.90% for Norit RX3 EXTRA. The experimental value of iron increment per repetition is about 40% of calculated values for both GACs. Most likely some of impregnated iron re-dissolved into the liquid phase in the following repetitions to cause the difference between experimental values and calculated values. This synthesizing method is easy to conduct and the iron content can simply be controlled by the number of repetitions. After 10 repetitions, 12.62% and 8.52% iron were impregnated in Darco 20×50 and Norit RX3 EXTRA, respectively. More iron may be impregnated with more repetitions.

Stability of Impregnated Iron

Iron desorption tests were carried out firstly to examine the stability of impregnated iron and results indicated that without post-treatment some of impregnated iron was unstable. Depending on iron content of Fe-GACs, 6-46% of impregnated iron were lost in desorption tests. EDS analysis revealed that large amounts of chlorine in Fe-GACs (Figure 2.a), which implied the existence of ferric or ferrous chlorides. Ferric and ferrous chlorides may dissolve into solution because ferric chloride and ferrous chloride have solubility of 92 g/100 mL and 68.5 g/100 mL in water at 20 °C, respectively.

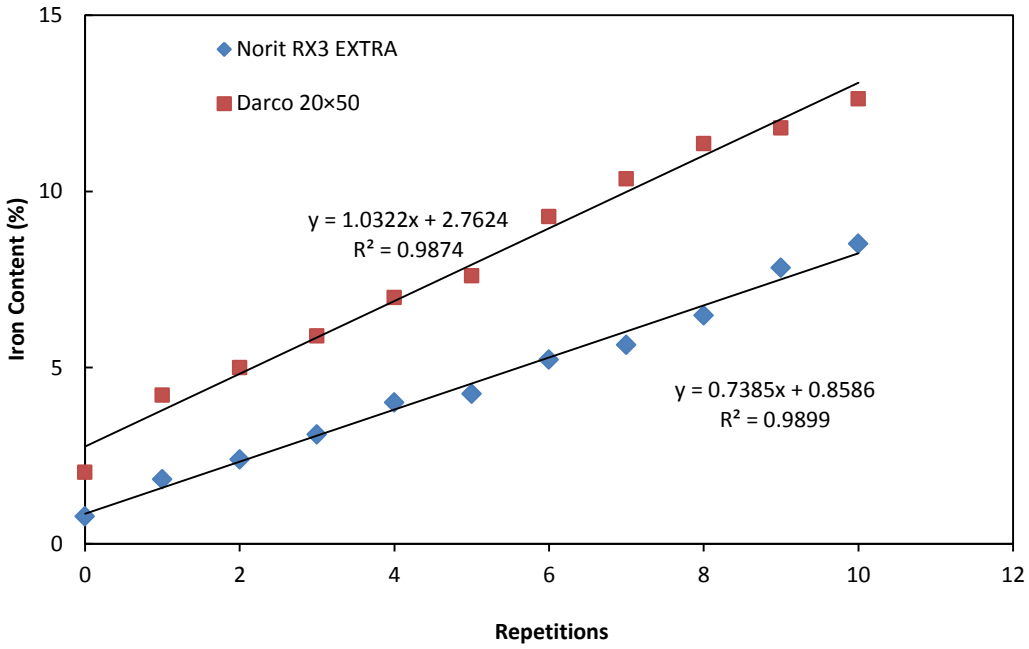

Figure 1. Increment of iron content with repetitions in the synthesis process.

A post-treatment was designed to further stabilize impregnated iron through conversion of iron chlorides to ferric hydroxide which is sparingly soluble (Table 1). After post-treatment, desorption tests were conducted again and results showed that the post-treatment successfully stabilized iron in Fe-GACs. EDS analysis, conducted on post-treated Fe-GACs, indicated that the amounts of chlorine reduced significantly (Figure 2.b). The stability of impregnated iron was also tested on Fe-GAC with 4.22% iron in the adsorption test with pH variation of 2-11. As shown in Figure 3, impregnated iron dissolved when pH was below 4. At pH 2.08, dissolved iron concentration was 25 mg/L, which is equivalent to 21% of impregnated iron. Impregnated iron was very stable when pH was above 4. Because pH is usually neutral in water resources, no concern is necessary for the iron stability of Fe-GACs. The iron stability was also monitored in all adsorption tests using ICP and the dissolution of impregnated iron was negligible.

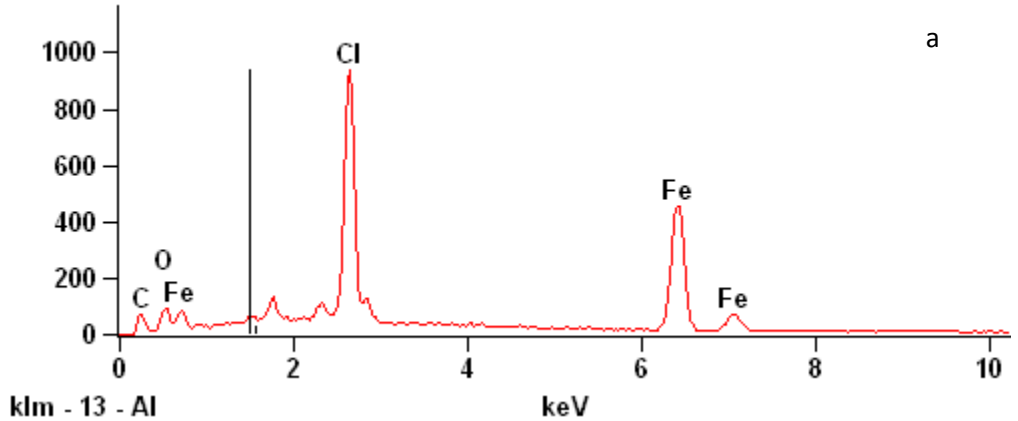

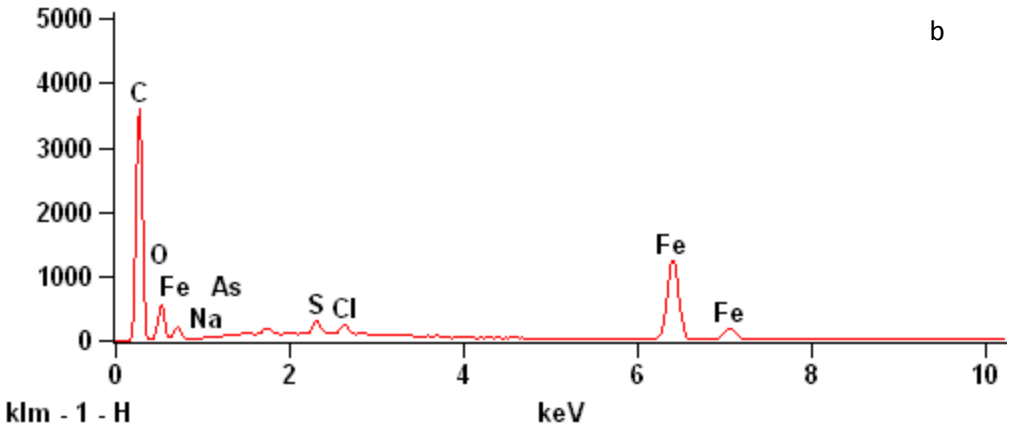

Figure 2. EDS spectra, a: Darco 20×50 Fe-GAC (12.68%) without post-treatment, b: Darco 20×50 Fe-GAC (9.29%) with post-treatment.

Table 1. Dissociation Constants of Iron Hydroxides

Iron Species	pK1	pK2	pK3	pKA
$Fe(OH)_3$ (Amorphous)	16.5	10.5	11.8	4.4
$Fe(OH)_2$	10.6	4.5	-	5.1

From Gunter Faure, 1998.

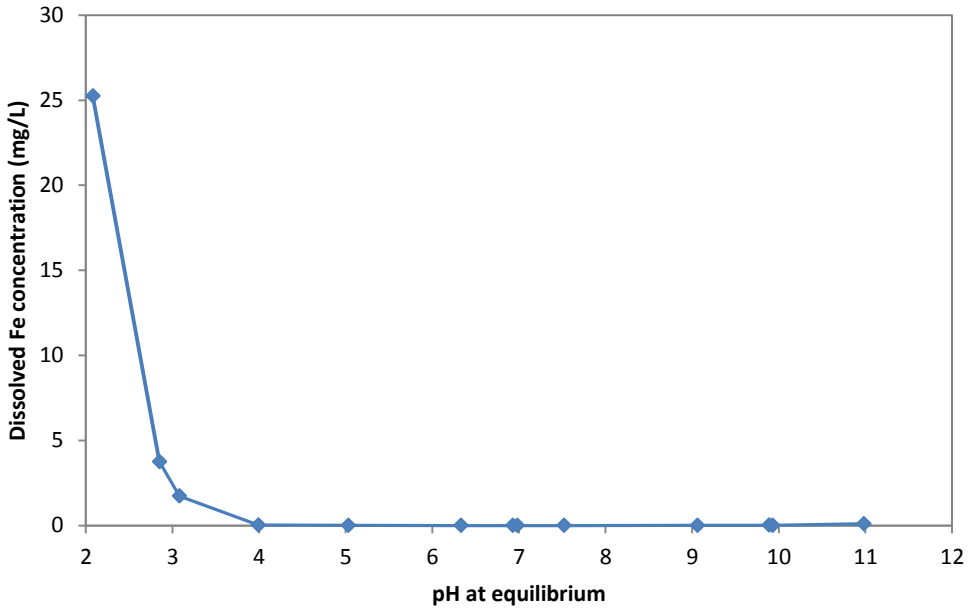

Figure 3. Stability of impregnated iron on Darco 20×50 Fe-GAC with 4.22% iron.

Characterization of Fe-GAC

Distribution of impregnated iron

Darco 20×50 Fe-GACs, with iron contents of 4.22%, 9.29% and 12.62%, were analyzed using SEM/EDS to investigate the iron distribution inside GAC. Figure 4 shows the relative weight percentages of iron in the four zones from the edge to the center on the cross-section of Fe-GACs (Figure 5), which indicated that iron was evenly distributed on the cross-section of GACs rather than concentrated on the edge. The variation of the iron relative weight percentages across the cross-section of Fe-GAC is likely caused by the heterogeneity of pore sizes and morphologies of GAC itself. The even iron distribution was found in Norit RX3 EXTRA Fe-GAC with iron content of 8.52 % as well.

As shown in Figure 4, relative weight percentages of iron are different between SEM/EDS analysis and the results from acid extraction method described in Section 3.2.3.1. With the acid extraction method as reference, SEM/EDS analysis generated underestimate at low iron content (4.22%), overestimate at high iron content (12.62%), and matched estimate with medium iron content (9.22%). EDS detects elements on the surface of samples with certain penetration depth. For Fe-GAC with low iron content, it is expected that iron distributed evenly on GAC internal surfaces in both macro-pores and micro-pores. Because most internal surface areas are contained in micro-pores and crosscutting of the Fe-GAC samples will not expose most micro-pores, EDS is not able to detect unexposed iron in micro-pores and resulted in underestimated iron contents. At high iron contents, iron crystals or nano-scale iron deposits may form in macro-pores. Exposure of large amount of iron in macro-pores could be the reason for overestimation of iron content from EDS analysis. (More EDS analyses are included in Appendix VI and VII)

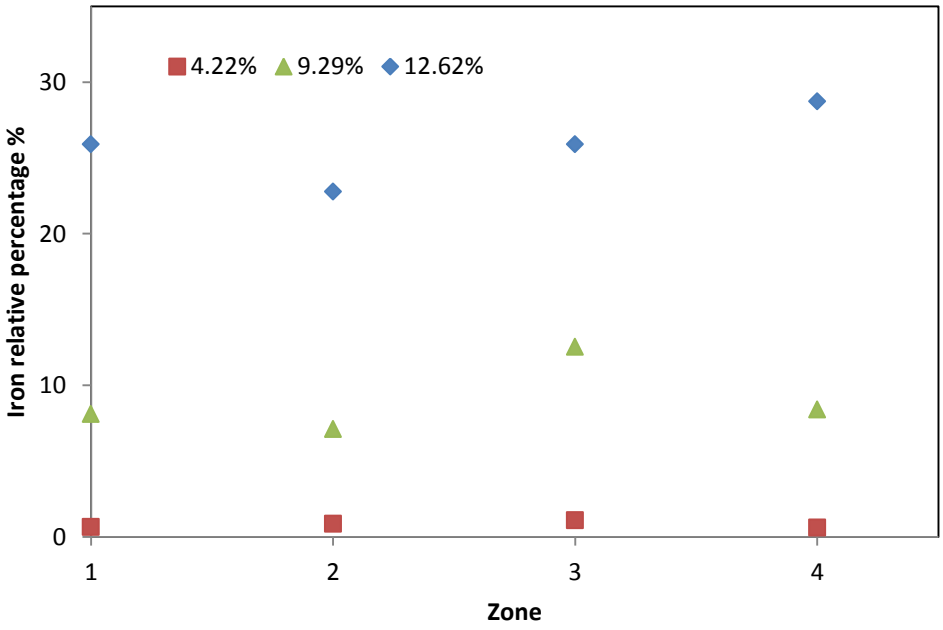

Figure 4. Iron distribution on the cross-section of Darco 20×50 Fe-GACs.

In addition to EDS analysis, mapping of iron distribution on the cross-section of Darco 20×50 Fe-GAC with 9.29% iron shows that impregnated iron covered the entire cross-section of Fe-GAC and higher iron content was observed in the macro-pores (cracks) of Fe-GAC (Figure 6).

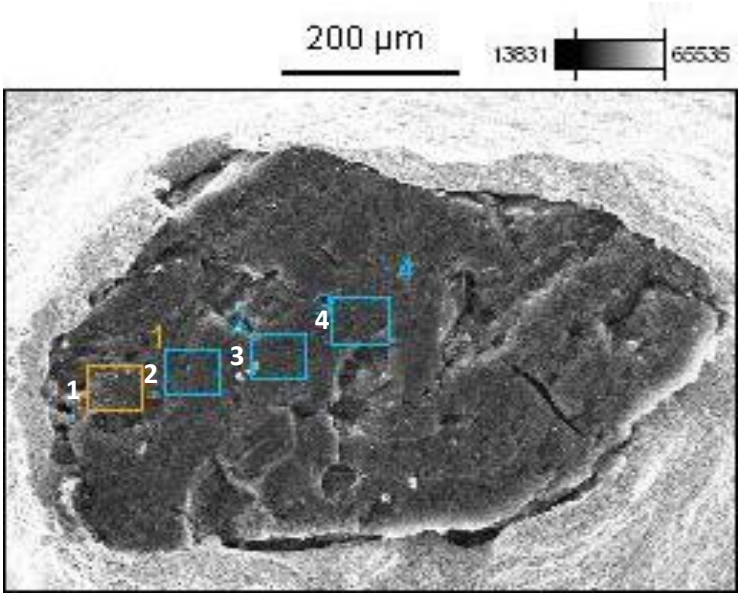

Figure 5. EDS analysis on the cross-section of Darco 20×50 Fe-GAC with 4.22% iron.

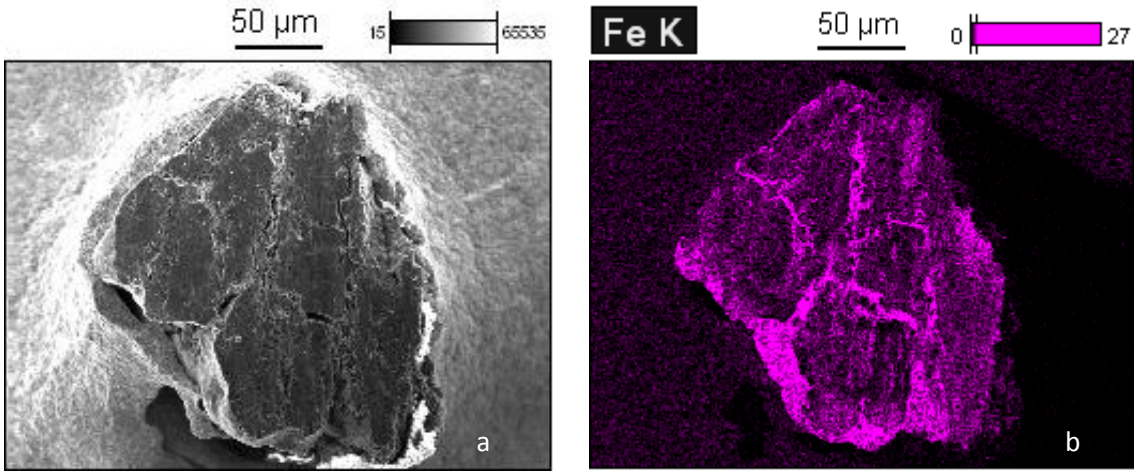

Figure 6. Mapping of iron distribution on cross-section of Darco 20×50 Fe-GAC with 9.29% iron. a:the cross-section of Fe-GAC; b: the mapping of iron.

Morphology of impregnated iron

Internal structure and morphology of Norit RX3 EXTRA Fe-GAC with 8.52% iron are shown in Figure 7. Iron formed rod-shape nano-size particles in macro-pores of GAC. In Figure 7b, iron rods were measured approximately 300 nm in length and 40 nm in diameter. Areas without iron rods in Figure 7a are believed to be areas with micro- and meso-pores which can be seen from lower left part of Figure 7b. Due to the constraint of pore size, impregnated iron

cannot form rod-shape nano-particles in these areas; however, iron is believed to exist in a smaller scale. Figure 8 shows morphologies of virgin and iron impregnated Darco 20×50 GAC. Instead of rod-shape nano-particles, irregular shapes of iron deposited in Darco 20×50 Fe-GAC with low iron content (Figures 8b and 8c) while nano-iron crystals were observed in Fe-GAC with high iron content (Figure 8d).

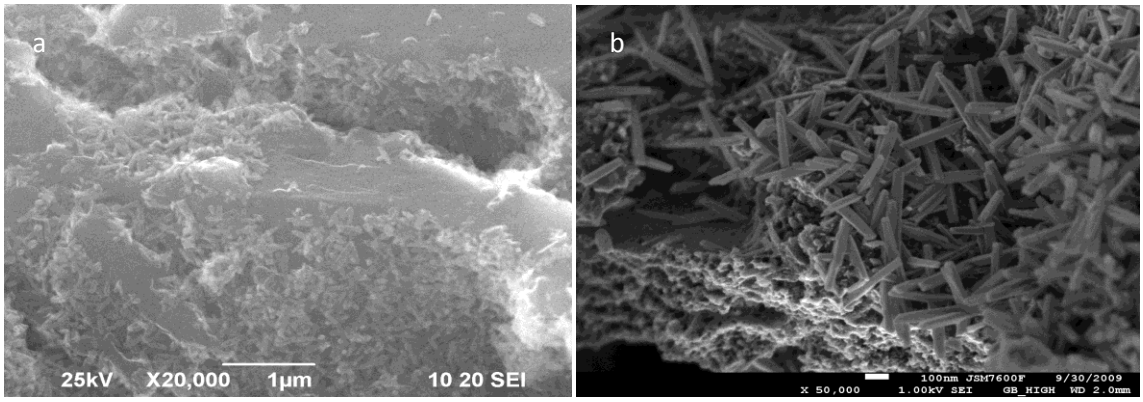

Figure 7. SEM images of Norit RX3 EXTRA Fe-GAC with 8.52% iron.

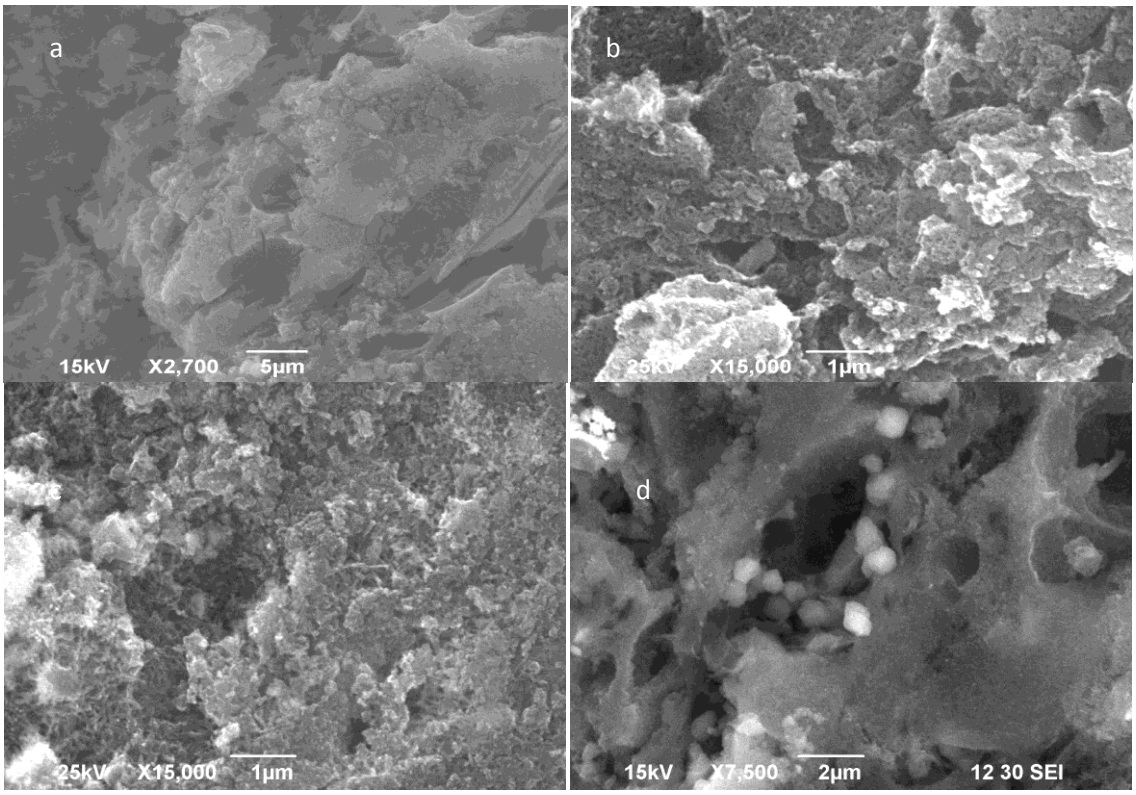

Figure 8. SEM images of Darco 20×50 Fe-GACs (a: virgin GAC; b: 4.22%; c: 9.29%; and d: 12.62%).

Iron species

Both post-treated and non-post-treated Fe-GACs were pulverized for XRD analyses to identify iron species. The major peaks of processed XRD spectra (Figure 9) matched well with the crystalline iron species akaganeite (β-FeOOH); while, the raw XRD spectrum (Figure 10) implies that significant amounts of amorphous iron existed in Fe-GAC as well. The species of impregnated iron are affected by impregnation methods and synthesizing conditions (*22, 28*). Jang et al. (*22*) reported that impregnated iron formed akaganeite at synthesizing temperature 80 °C and amorphous hydrous ferric oxide (HFO) at 60 °C. However, Gu et al. (6) found that impregnated iron in GAC, synthesized at 80 °C, were all in amorphous state. Results of this study found that impregnated iron existed as both crystalline and amorphous species in GAC.

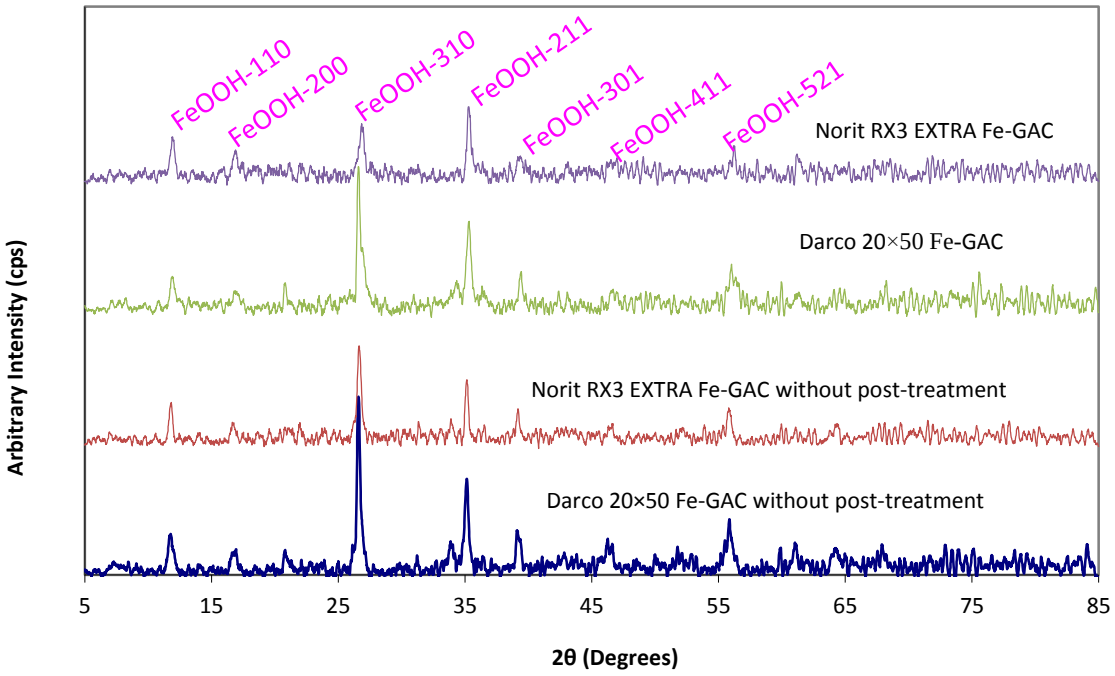

Figure 9. XRD spectra of Fe-GACs.

pH Impact on Arsenic Adsorption

pH is one of the most important factors affecting arsenate adsorption in the liquid phase (*6,14,15, 22,29*), because the arsenate species and the surface charge of Fe-GACs in liquid phase depend on pH. The impact of pH on arsenate removal was studied with pH values ranging from 2 to 11 using 100 mg Darco 20×50 Fe-GAC with 4.22% iron and 35 mL 3 mg/L arsenate solution. As shown in Figure 11, arsenic removal rate maintained close to 100% at pH 2-6 and declined slightly at pH 6.0-7.0. When pH was above 7.0, arsenic removal rate declined quickly. To minimize the impact of pH variation on isotherm tests as well as to keep experimental conditions close to natural waters, the pH in arsenate isotherm tests was controlled at 7.0 using bicarbonate buffer solution.

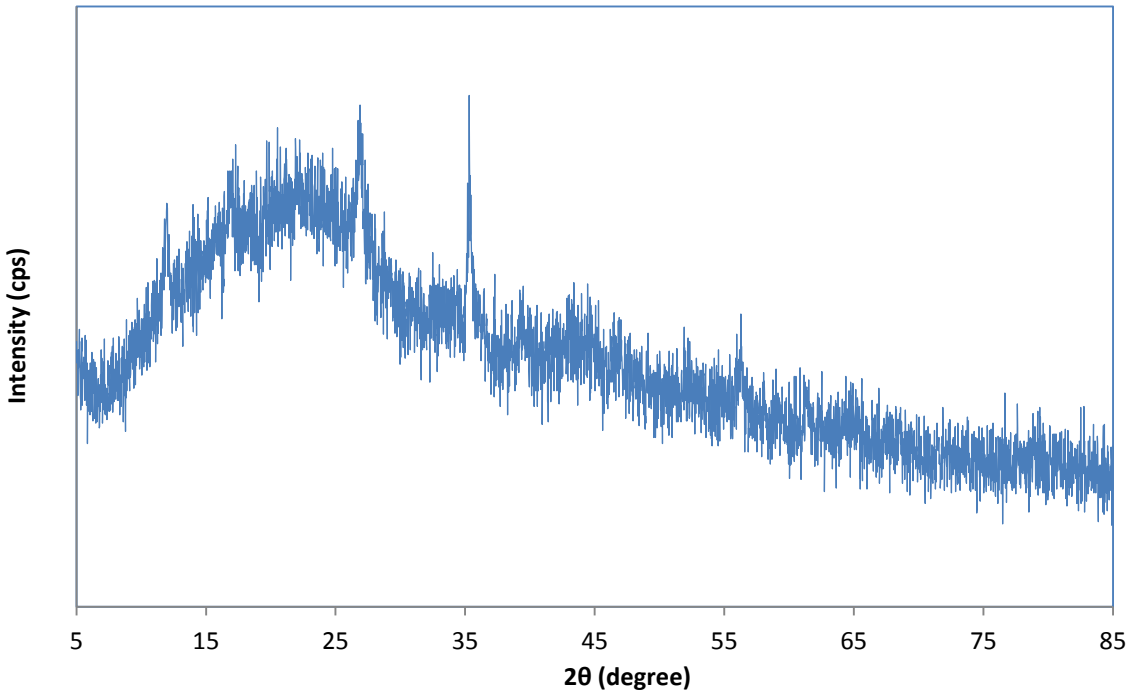

Figure 10. Raw XRD spectrum for Norit RX3 EXTRA Fe-GAC with post-treatment (Iron content 7.53%).

To evaluate the impact of pH on arsenate adsorption, major arsenate species in different pH ranges are included in Figure 11. Arsenate species in aqueous phase exist mainly as H_3AsO_4 at pH less than 2.2 (pK_1), $H_2AsO_4^-$ at pH between 2.2 and 6.98 (pK_2), $HAsO_4^{-2}$ at pH between 6.98 and 11.5 (pK_3), and AsO_4^{-3} at pH above 11.5. pH_{zpc} is the pH at which adsorbents have a net zero surface charge (*30, 31*). The pH_{zpc} for Fe-GAC was between 8.2 and 8.7 (*15*). As shown in Figure 11, Fe-GACs becomes more positively charged when pH is less than 8.3 (pH_{zpc}) and more negatively charged when pH is above 8.3. As pH increased, the attractive force between Fe-GAC and arsenate became less and changed to repulsive force when pH above 8.3. The change of the electrostatic force between arsenate species and Fe-GAC explained the pH impact on arsenate adsorption.

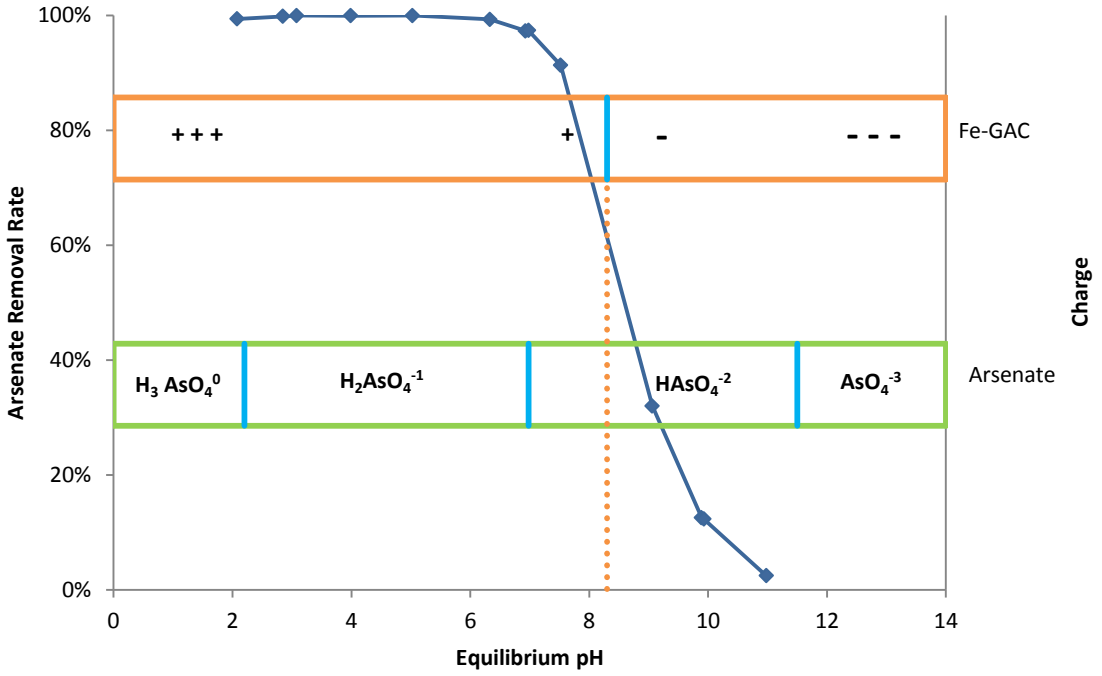

Figure 11. Impact of pH on arsenic adsorption on Darco 20×50 Fe-GAC with 4.22% iron.

Arsenic Adsorption Equilibrium Time

Adsorption rate and time required for reaching equilibrium are a function of several factors, including activated carbon particle size, pore structure and adsorbate characteristics (*30*). It may take a few hours to reach equilibrium for adsorption of contaminants with small molecular sizes on powered or pulverized activated carbons, while few months may be necessary for adsorption of larger molecules on GAC to reach true equilibrium (*30, 32*). Impregnation of iron on GAC not only changes the GAC surface characteristics in favor of arsenic adsorption, but also alters the GAC pore sizes and structures. Reduction of pore size and pore volume of activated carbon due to iron impregnation has been documented by several research groups (*6, 14, 23*). Volume reduction was found to be linearly related to the amount of iron content and it was speculated that iron particles may block or partially block some of the pores making them not available for arsenic removal or slowing the adsorption process.

Because intraparticle diffusion rate and overall arsenic adsorption kinetics are likely affected by iron impregnation, longer equilibrium time may be required for Fe-GAC with high iron contents. Therefore, it is necessary to find an adequate adsorption duration for reaching adsorption equilibrium so that the impact of iron content on arsenic adsorption capacity can be properly evaluated. Fe-GACs with five different iron contents ranging from 5.57% to 28.90% were used to study As(V) removal versus adsorption time. Experiments were run for 15 days with samples taken at predetermined intervals for arsenic analysis. Amount of arsenic adsorbed at each sampling time was normalized by the adsorption capacity at 15 days and results are presented as percentage of adsorption capacity in Figure 12. Arsenic removal occurred rapidly in

the first 24 hours, reaching 80% or higher of the maximum capacities for all Fe-GACs. Much slower removal rates were observed afterward. It took 48 hours to reach 90% of total capacities and 120 hours to achieve 95%. It is also observed that adsorption on each Fe-GAC proceeded at different rates and the difference is most noticeable during first 24 hours (see Figure 12 insert). In general, Fe-GACs with higher iron contents exhibits slower arsenic removal rate. This may be explained by slower arsenic intraparticle diffusion rate due to the GAC pore size reduction from iron impregnation. Figure 12 shows that the percentage of total adsorption capacity realized is getting close to each other for Fe-GACs with different iron contents after 24 hours. It has to be noted that a small percentage difference in total adsorption capacity for Fe-GACs with high iron contents may represent significant capacity for arsenic removal, because the total (maximum) arsenic adsorption capacities for different iron contents (presented later in this paper) are different, Based on the results of this study and practical consideration, a 5-day adsorption time was selected for arsenic adsorption isotherm tests in this study.

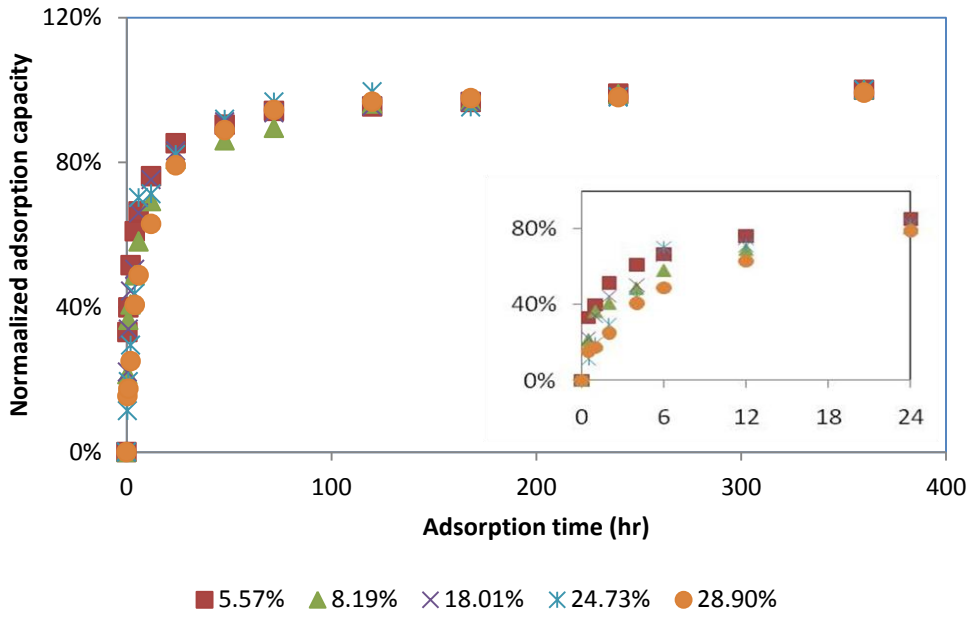

Figure 12. Impact of adsorption time on arsenic adsorption for Fe-GACs with different contents.

As(III) and As(V) Adsorption Isotherms

Fe-GACs with eleven iron contents ranging from 1.64% to 28.90% were tested to investigate the impact of iron contents on arsenic adsorption properties at a low concentration range (<250 µg/L) which is typical in contaminated drinking water sources. Contaminated water sources may contain both As(III) and As(V). Therefore, both As(III) and As(V) were tested in isotherm tests. The pH of adsorption isotherm tests was controlled in a narrow range to minimize its impact .

As shown in Figures 13 and 14, As(V) and As(III) adsorption capacities on Fe-GACs were enhanced significantly with increase of iron content. Virgin GAC was tested as well, while the result is not presented in Figure 13 due to its negligible arsenic adsorption capacity.

Langmuir model (Eq. 2) was chosen to interpret the experimental data because the nature of arsenic adsorption on Fe-GAC is site specific adsorption (*33*, *34*). In order to avoid biased estimates from linearization of Langmuir model, a non-linear least squares regression procedure was developed using Statistical Analysis System (SAS) to estimate the parameters in Langmuir model (*12*). Langmuir parameters obtained from the best fits of As(V) and As(III) experimental data are shown in Table 2 and model simulations are shown as solid lines in Figures 13 and 14. As shown in Table 1 and Figures 13 and 14, Langmuir model fits As(V) and As(III) adsorption equilibrium data well with correlation coefficient (R^2) of 0.96 or better.

$$q = q_m \frac{b \cdot c_e}{1 + b \cdot c_e} \qquad (2)$$

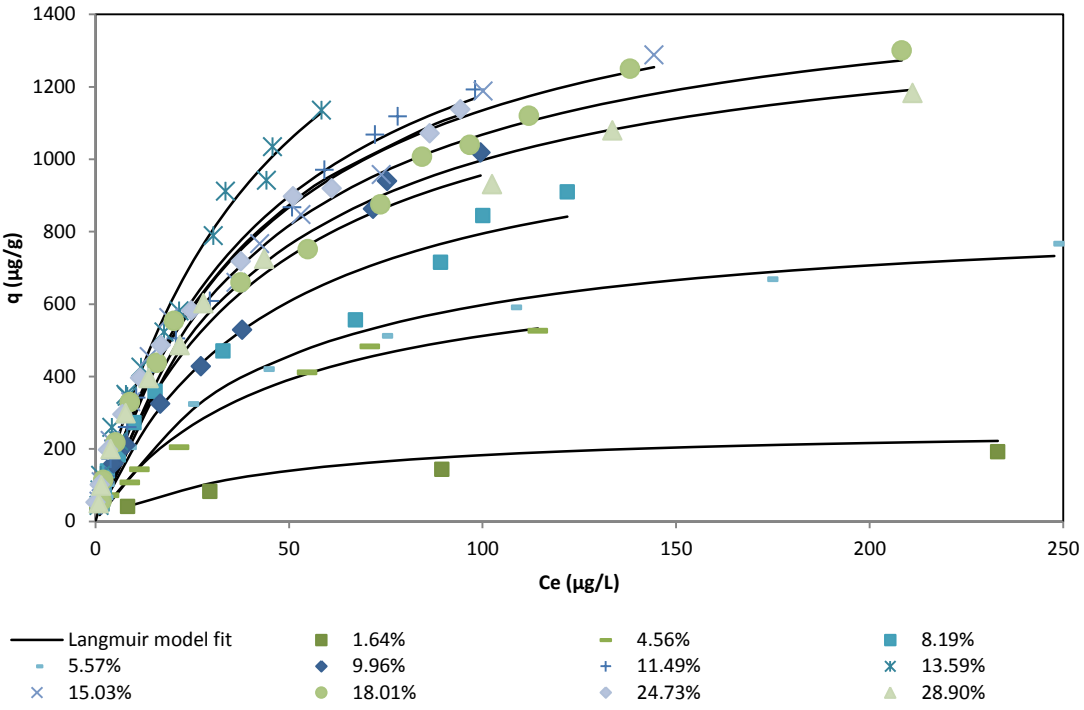

Figure 13. As(V) adsorption isotherm curves for Fe-GACs with different iron contents.

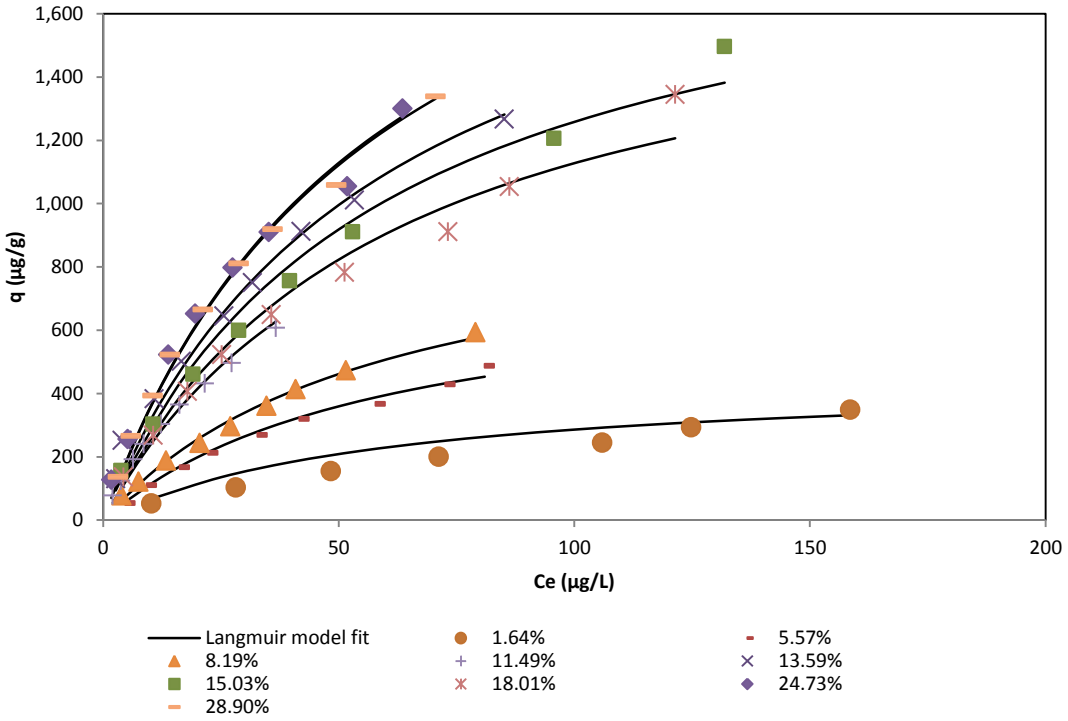

Figure 14. As(III) adsorption isotherm curves for Fe-GACs with different iron contents.

Table 2. Langmuir Model Parameters for As(III) and As(V) Adsorption on Fe-GACs

Iron content (%)	As(V)				As(III)			
	pH	q_m (µg/g)	b (L/µg)	R^2	pH	q_m (µg/g)	b (L/µg)	R^2
1.64	7.30	304	0.0097	0.9740	7.11	893	0.0040	0.9907
4.56	7.33	795	0.0190	0.9899	/	/	/	/
5.77	7.24	562	0.0259	0.9763	7.18	878	0.0138	0.9917
8.19	7.23	827	0.0263	0.9556	6.86	1112	0.0143	0.9956
9.96	7.41	1061	0.0282	0.9857	/	/	/	/
11.49	7.24	1912	0.0116	0.9927	6.98	1109	0.0311	0.9958
13.59	7.37	1776	0.0204	0.9828	6.93	1922	0.0214	0.9877
15.03	7.20	1867	0.0252	0.9776	7.12	2350	0.0122	0.9928
18.01	7.22	1591	0.0243	0.9809	7.36	2170	0.0116	0.9842
24.73	7.20	1550	0.0222	0.9865	6.87	2037	0.0239	0.9878
28.90	7.20	1495	0.0286	0.9895	7.38	2181	0.0208	0.9952

The symbol of / indicates that the experimental data is not available.

Adsorption Affinity of Arsenic on Fe-GACs

The parameter *b* in the Langmuir model represents the affinity of an adsorbate to an adsorbent. From the reaction kinetics aspect, the parameter *b* in Langmuir model is the ratio of the adsorption rate constant to desorption rate constant (*32, 35*). According to the reaction thermodynamics, the parameter *b* is related to the net enthalpy of adsorption that reflects the strength of binding of the adsorbate to the adsorbent (*30, 36, 37*). Therefore, higher *b* value indicates higher adsorption affinity that means most adsorption capacity can be utilized at low equilibrium concentration (*12*). As shown in Tables 2, the values of parameter *b* vary in a narrow range for Fe-GACs with different iron contents, except for iron content of 1.64%. The average *b* value and the standard deviation are 0.0223±0.006 L/μg for As(V) and 0.0170±0.008 L/μg for As(III), respectively. Because Fe-GACs in this study were synthesized by the same procedure, the surface characteristics of impregnated iron are expected to be the same. The Langmuir constant *b* is, therefore, expected to be the same for Fe-GACs with different iron contents. Based on the above consideration, a hypothesis was postulated that the amounts of impregnated iron of Fe-GACs only affect the arsenic maximum adsorption capacities but not the affinity for arsenic.

To determine whether the isotherm data support this hypothesis, the non-linear regression process was repeated with the same *b* value for all Fe-GACs with different iron contents. The average *b* values for As(V) and As(III) adsorptions were used as common values in the non-linear regression. Results of this analysis show that Langmuir model with the same parameter *b* value can still well fit the adsorption isotherms for both As(III) and As(V) (Table 3). This verifies that Fe-GACs with different iron contents possess the same affinity for arsenic.

Table 3**. Re-estimated q_m in Langmuir Model with same *b* Values for As(III) and As(V) Adsorption on Fe-GACs**

Iron content (%)	As(V)			As(III)		
	q_m (μg/g)	b (L/μg)	R^2	q_m (μg/g)	b (L/μg)	R^2
1.64	265	0.0223	0.9183	454	0.0170	0.8753
4.56	742	0.0223	0.9883	-	-	-
5.77	866	0.0223	0.9744	782	0.0170	0.9893
8.19	1151	0.0223	0.9533	1004	0.0170	0.9938
9.96	1385	0.0223	0.9701	-	-	-
11.49	1703	0.0223	0.9920	1634	0.0170	0.9806
13.59	1996	0.0223	0.9823	2166	0.0170	0.9843
15.03	1644	0.0223	0.9772	1998	0.0170	0.9842
18.01	1547	0.0223	0.9809	1791	0.0170	0.9752
24.73	1657	0.0223	0.9831	2456	0.0170	0.9813
28.90	1445	0.0223	0.9818	2441	0.0170	0.9927

It is noticed that Fe-GAC with iron content of 1.64% has the poorest Langmuir model fits for both As(III) and As(V) in Table 3, which implies that Fe-GAC with iron content of 1.64%, as a whole adsorbent, presents very different surface characteristics from others. This is probably because the iron content of 1.64% is so low that only a small fraction of the surface of GAC is covered by iron. The overall surface characteristics of Fe-GAC with iron content of 1.64% are mainly determined by the bare surface of GAC that has very low affinity for arsenic adsorption. When much higher affinity is assigned to Fe-GAC with iron content of 1.64%, poor Langmuir model fit is anticipated.

Parameter q_m of Langmuir model is commonly used to evaluate and compare arsenic adsorption of Fe-GACs produced from different GACs and impregnation methods in literature (*6, 38-41*). The parameter *b*, however, draws less attention even though it has significant influence on adsorption capacity at low equilibrium concentrations. The adsorption affinity of Fe-GACs synthesized in this study, 0.0223 L/μg for As(V) and 0.0170 L/μg for As(III), are comparable or higher than the values reported in literature (*6, 8, 16*), indicating that Fe-GACs synthesized in this study are suitable for applications on arsenic contaminated drinking water. High affinity of arsenic to Fe-GACs observed in this study probably is attributed to two reasons: the favored surface characteristics of impregnated iron and low arsenic concentration in isotherm tests. XRD analysis on Fe-GAC samples showed that the dominating iron species on GAC surfaces is akageneite, which is considered one of the most favored hydrous ferric oxide species for arsenic removal (*33*). Authors identified an interesting observation in literature that that the statistical regression analysis on Langmuir model tends to return high q_m and low b when isotherm tests were conducted at high equilibrium concentration, while low q_m and high b at low equilibrium concentrations (*8, 29, 42*). This study intends to evaluate the adsorption properties of Fe-GACs at conditions close to real cases, usually low arsenic concentration. Therefore, the isotherm test conditions may contribute to high *b* values in Langmuir model analysis.

Impact of Iron Content of Fe-GACs on Arsenic Adsorption Capacities

The arsenic maximum adsorption capacity, q_m, was used to evaluate the impact of the iron content of Fe-GACs on the arsenic adsorption capacity because q_m is independent of the arsenic equilibrium concentration. As shown in Table 3 and Figure 15, q_m for As(V) increased from 265 μg/g to 1996 μg/g when impregnated iron increased from 1.64% to 13.59%. Then, the q_m gradually decreased to 1445 μg/g with impregnated iron increasing to 28.90%. For As(III), q_m quickly increased from 454 μg/g to 2116 μg/g when impregnated iron increased from 1.64% to 13.59%. Further increase of iron contents resulted in slower increase of q_m, which reached 2456 μg/g at iron content of 24.73%. As shown in Figure 15, when iron content is below 13.59%, the q_m for both As(III) and As(V) increased linearly with iron content and are at approximately same values. This is probably because the adsorption sites on Fe-GACs are accessible to both As(III) and As(V), and the number of adsorption sites is proportional to the amount of impregnated iron. When iron content is higher than 13.59%, adsorption capacity is compromised by partial blockage of pore structures or covering up adsorption sites (detailed explanation in the next section). Similar observations were documented in the previous studies (*6, 23*). It is speculated that the accessibility of adsorption sites is different for As(III) and As(V) due to the different chemical properties and physical size of these two arsenic species on Fe-GACs with high iron contents.

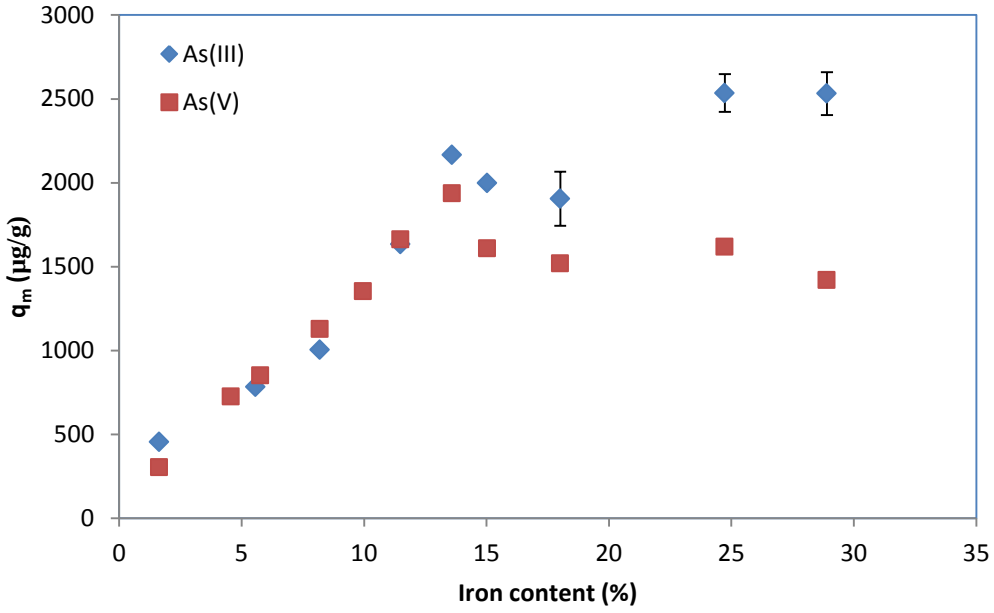

Figure 15. Maximum adsorption capacities of Fe-GACs for As(III) and As(V)

BET Surface Area and Pore Structures of Fe-GACs

Pore size distribution and BET surface area of Fe-GACs were analyzed to investigate the impact of iron content on arsenic adsorption capacities. Fe-GACs with iron content of 0-28.90% were selected for the analysis of BET surface area and pore structure. Figure 16 shows the BET surface area of Fe-GAC ($S_{Fe\text{-}GAC}$) decreased from 554 m^2/g to 308 m^2/g as the iron content increased from 0% (virgin GAC) to 28.90%. The average deduction of $S_{Fe\text{-}GAC}$ per percent of impregnated iron is 6 $m^2/g \cdot$%Fe, less than 20-34 $m^2/g \cdot$%Fe reported in literature (*6, 16*). The smaller deduction rate of $S_{Fe\text{-}GAC}$ implies that impregnated iron is evenly distributed on the internal surface area of GAC. $S_{Fe\text{-}GAC}$ is usually used to explain the arsenic adsorption capacity in literature because it is readily reported from the instrumental analysis. However, $S_{Fe\text{-}GAC}$ contains the surface area of both impregnated iron and GAC and cannot be directly related to arsenic adsorption capacity because the surface area of impregnated iron (S_{Fe}) determines arsenic adsorption capacity.

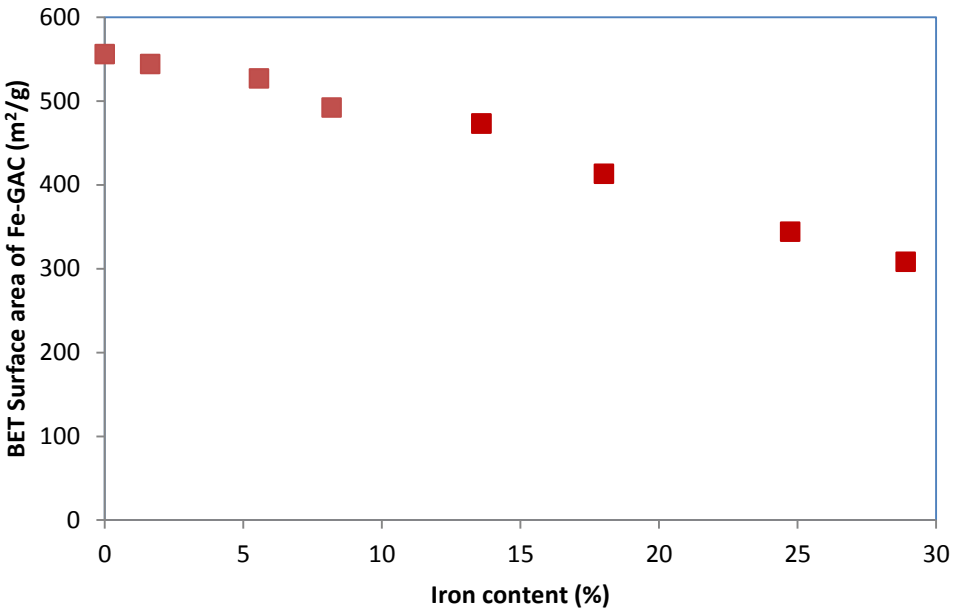

Figure 16. BET surface area of Fe-GACs with different iron contents.

S_{Fe} can be estimated from $S_{Fe\text{-}GAC}$ and their relationship changes with iron contents. When a small amount of iron is impregnated in GAC, iron (in this case akaganeite) generate active surface for arsenic adsorption. At the same time, internal surface area of GAC is covered and the pore volume is occupied by impregnated iron, which causes an overall deduction of $S_{Fe\text{-}GAC}$. At low iron contents, S_{Fe} increases with increase of iron content, while $S_{Fe\text{-}GAC}$ decreases. When the internal surface of GAC is fully covered by iron and a maximum S_{Fe} is reached, S_{Fe} is equal to $S_{Fe\text{-}GAC}$ and further increase of iron will result in decrease of both $S_{Fe\text{-}GAC}$ and S_{Fe}. Because adsorption capacity of arsenic is proportional to S_{Fe}, q_m will increase with increase of S_{Fe} and decrease with decrease of S_{Fe}. Based on the above considerations and the highest q_m obtained at iron content of 13.59%, it is assumed that the impregnated iron fully covers the internal surface area of GAC and reached a maximum S_{Fe} at iron content of 13.59%. Therefore, in the range of 0-13.59%, S_{Fe} increases with iron content while $S_{Fe\text{-}GAC}$ decreases with iron content. In the range of 13.59-28.90%, both S_{Fe} and $S_{Fe\text{-}GAC}$ decrease with iron content.

With the assumption that impregnated iron fully covers the internal surface of GAC at 13.59%, S_{Fe} was calculated for Fe-GACs with different iron contents. Then, the q_m was calculated based on the iron content, S_{Fe}, and arsenic specific adsorption density. Comparison of calculalted q_m with experimental value in Figure 17 shows that the calculated As(V) q_m agreed with the experimental data well, which verified the assumption that the internal surface of GAC is fully covered by impregnated iron at iron content of 13.59%. This assumption was confirmed by the same analysis on As(III) as well.

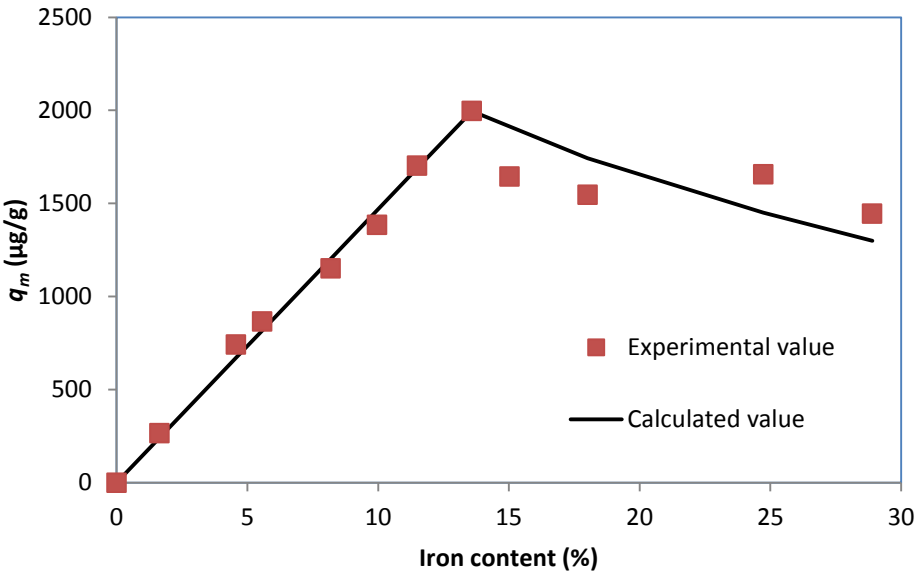

Figure 17. Comparison of calculated As(V) maximum adsorption capacity with experimental value

Figure 18 depicts the relationship between the As(V) adsorption density, defined as ratio of q_m to iron content of Fe-GAC), and S_{Fe}. As show in Figure 18, As (V) adsorption density remains at approximately the same level before GAC is fully covered with impregnate iron (S_{Fe} 473 m^2/g at iron content of 13.59%). Then, as iron content keeps increasing (> 13.59%), arsenic adsorption density decreased with decreasing of S_{Fe} because of the formation of multi-layer of impregnated iron.

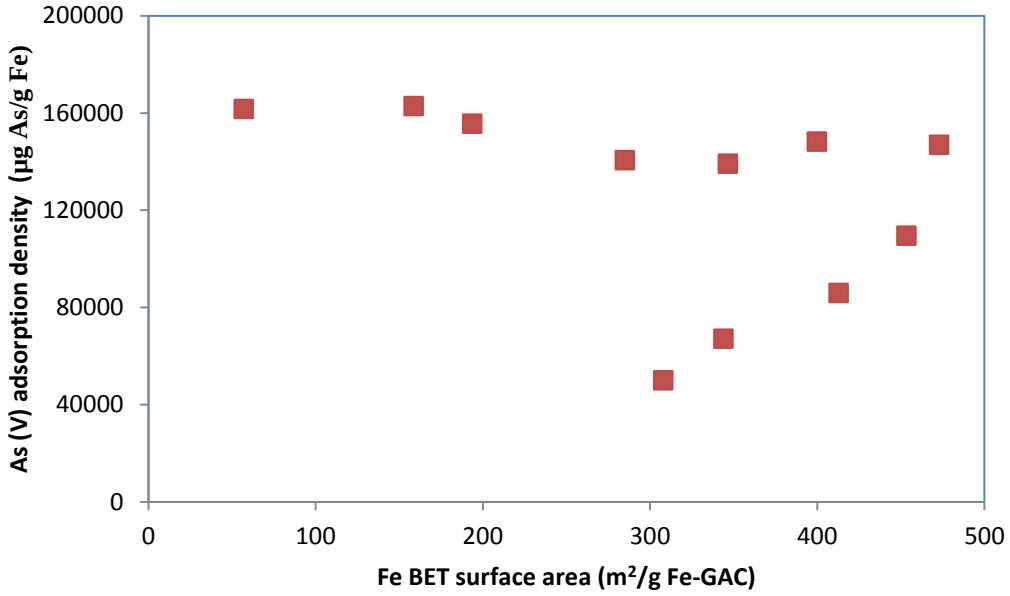

Figure 18. As(V) maximum adsorption capacity vs. S_{Fe}

Figure 19 shows the distribution of $S_{Fe\text{-}GAC}$ with pore size, which indicates that more than 73% of $S_{Fe\text{-}GAC}$ was contributed from pores with size less than 2 nm in the tested range of pore size (< 40nm). This is consistent with the finding in the kinetic study that long adsorption time is necessary to reach the adsorption equilibrium.

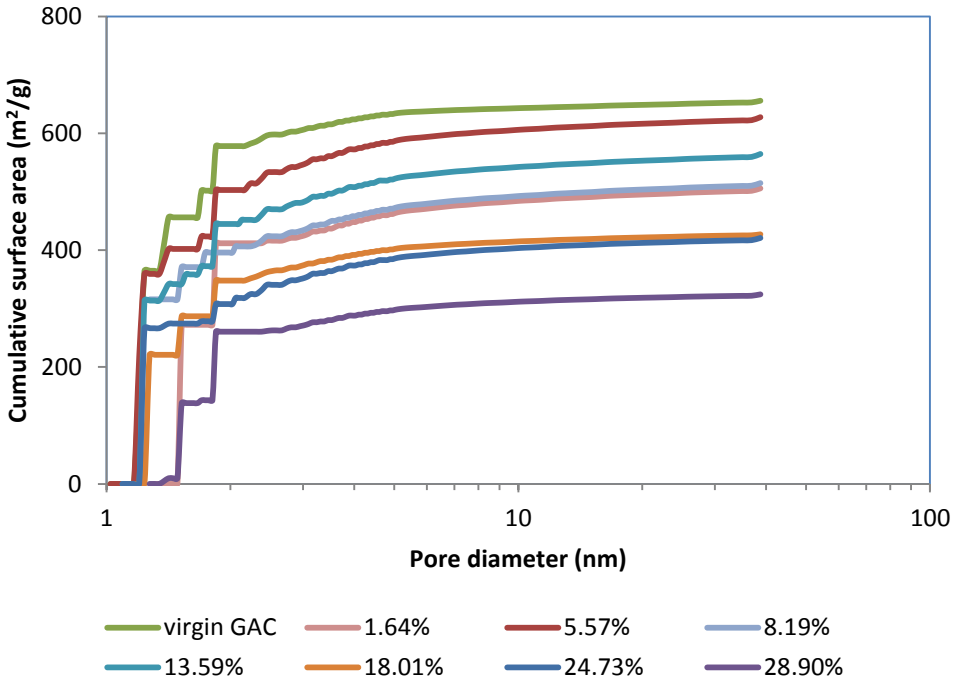

Figure 19. Distribution of surface area of Fe-GACs with pore size.

The pore volume of Fe-GACs reduced linearly from 0.711 cm^3/g to 0.299 cm^3/g when iron content increased from 0% to 28.90% (Table 4), which implies that the density of impregnated iron are for Fe-GACs with different iron contents. This agrees with the finding in the arsenic isotherm tests that the surface characteristics of impregnated iron are the same for Fe-GACs. With iron impregnation, the average meso-pore size of Fe-GACs continuously reduced from 9.95 nm to 7.48 nm, which may explain why the initial arsenic adsorption rate decreased with more impregnated iron (Figure 12).

Table 4. Texture Parameters for Fe-GACs and Virgin GAC

Iron content (%)	$S_{Fe\text{-}GAC}$ (m^2/g)	Pore Volume (cm^3/g)	Average pore diameter (nm)
Virgin GAC	556	0.711	9.95
1.64	544	0.634	9.04
5.57	527	0.612	9.17
8.19	492	0.606	9.22

13.59	473	0.533	8.84
18.01	413	0.436	8.12
24.73	344	0.356	7.99
28.90	308	0.299	7.48

Application for Arsenic Removal from Groundwater

The groundwater sample was taken from the former Arsenic Trioxide Superfund site (Site ID #0800522) in southeastern North Dakota for the evaluation of the potential implementations of Fe-GACs. The average arsenic concentration in the groundwater sample is 205 µg/L (Table 5) and the groundwater sample was spiked with As(V) to obtain an initial arsenic concentration of 3000 µg/L for isotherm tests. No other modification to the groundwater sample was made. As shown in Figure 20, Fe-GACs can effectively remove arsenic from the groundwater and the arsenic adsorption capacity was enhanced greatly with impregnated iron. Langmuir model can well fit arsenic adsorption on Fe-GACs with a common constant *b* of 0.0073 L/µg (Table 6)**.** Compared with isotherm tests using arsenic synthetic water (As(III) and As(V)), Fe-GACs exhibited the approximately same maximum adsorption capacity for groundwater, which is because the maximum adsorption capacity is determined by the density of adsorption sites of Fe-GACs. However, the affinity of Fe-GACs for groundwater is much less than these for As(III) and As(V) synthetic water. The presence of a large amount of phosphate in groundwater probably explains the lower affinity for arsenic (Table 5). Due to the similar molecular structure with arsenic, phosphate is the most competing anion with arsenic on iron-based adsorbents (*43-45*). In real implementations, the properties of other sorbates in groundwater must be considered as well. This research is in the process of testing the arsenic removal in Fe-GAC packed columns and findings will be reported in the following publication.

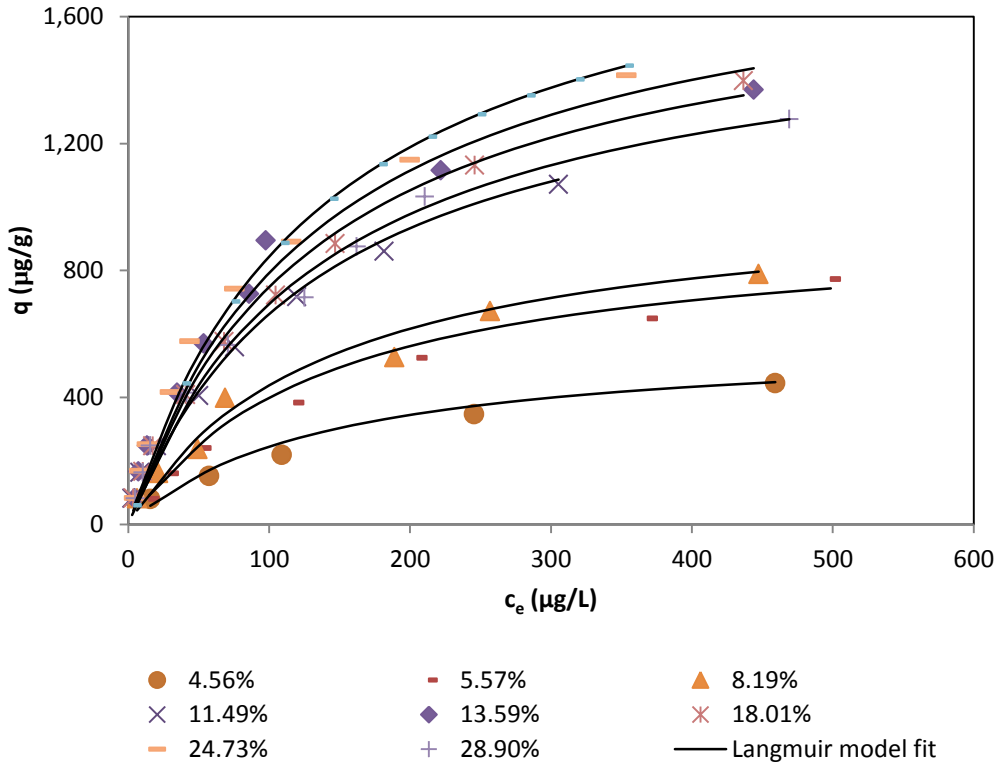

Figure 20. Adsorption isotherm curves for As(V) spiked groundwater (lines are Langmuir model with the same b values).

Table 5. Water Quality of Groundwater

Items	Value
Arsenic	205 µg/L
pH	7.50
Total P	167 µg/L
TOC	1.28 mg/L
Specific conductivity	1734 µs/cm
DO	3.32 mg/L
Temperature	5.9°C
Turbidity	2.40 NTU

Table 6. Langmuir parameters for groundwater isotherm tests with constant *b* at 0.0073 L/µg

Iron content (%)	pH	q_m (µg/g)	R^2
4.56	7.79	583	0.9853
5.57	7.69	949	0.9828
8.19	7.60	1042	0.9840
11.49	7.56	1577	0.9935
13.59	7.57	1883	0.9857
18.01	7.55	1779	0.9954
24.73	7.65	2008	0.9901
28.90	7.72	1652	0.9922

Effect of Iron Content on Arsenic Breakthrough

Based on arsenic isotherm tests, Fe-GACs with 8 different iron contents were chosen for column tests to investigate the impact of iron content on arsenic breakthrough. Breakthrough curves, plotted as c_{en}/c_{in} vs. bed volume (BV, defined as the ratio of the volume of influent treated to empty bed volume), are shown in Figure 21. The arsenic breakthrough concentration is set at 10µg/L, which is consistent with USEPA regulation on arsenic in drinking water (*4*). With increasing of iron content, Fe-GACs showed enhanced performance on arsenic removal in column tests.

As shown in Figure 21, Fe-GAC with 4.56% iron treated 140 BV at breakthrough. When iron content increased from 4.56% to 13.59%, BV treated at breakthrough increased from 140 to 1,000. When iron content is higher than 13.59%, BV treated at breakthrough varied between 850 and 950. To evaluate the efficiency of Fe-GAC in column tests, a Fe-GAC utilization rate was defined as the ratio of the BV treated at breakthrough to possible BV calculated based on arsenic adsorption isotherms (Eq. 3). Also shown in Figure 22, the utilization rate reduced with increase of iron content. With iron content increasing from 5.57% to 28.90%, the utilization rate reduced from 35% to 23%.

$$Fe - GAC\ Utilization\ rate = \frac{BV\ number\ treated\ at\ breakthrough}{Possible\ BV\ number\ calculated\ based\ on\ isotherm\ adsorption} \quad (3)$$

The performance of Fe-GACs in column tests is consistent with their performance in isotherm tests. Relationships between iron content and adsorpiton capacity/utilization rate in column tests show the same trends as relationships between iron content and maximum adsorption capacity/iron use efficiency in isotherm tests.

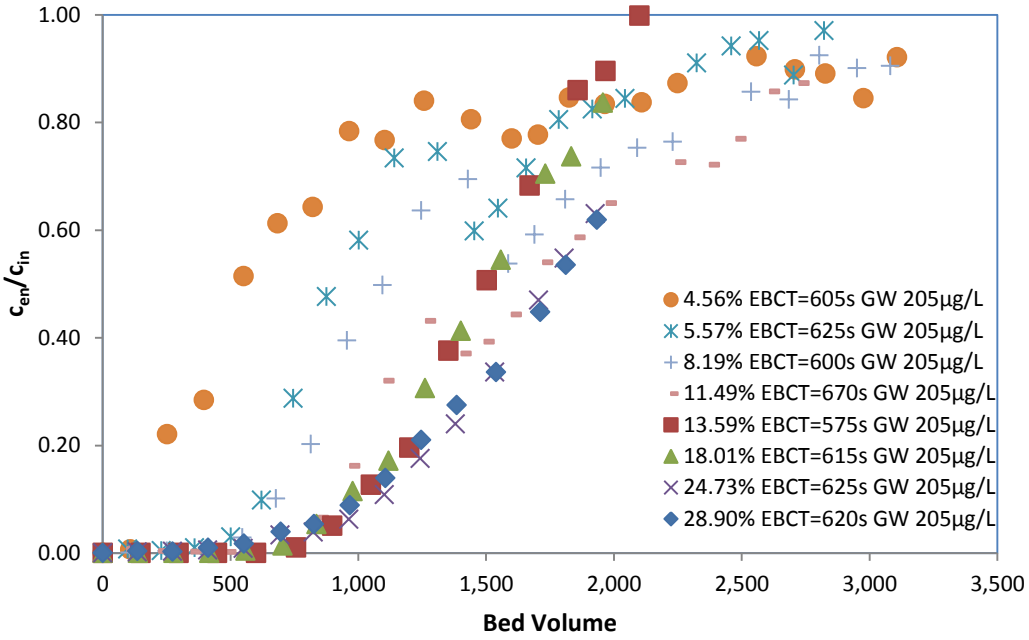

Figure 21. Breakthrough curves of Fe-GACs with EBCT 600 s.

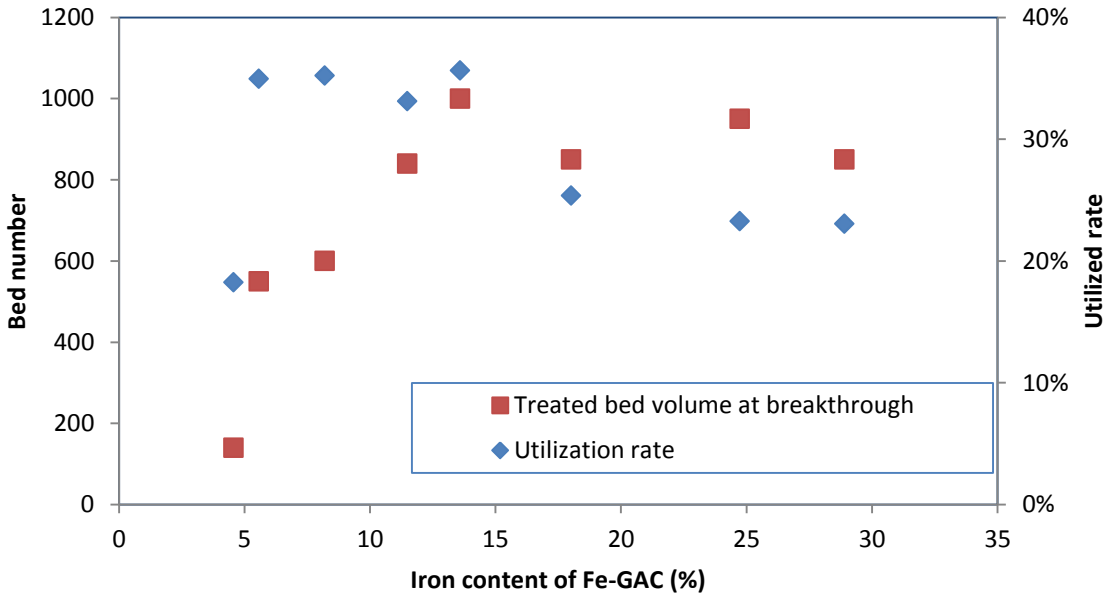

Figure 22. Relationship between iron content of Fe-GACs and BV treated/utilization rate at breakthrough.

In addition to the number of BV treated at breakthrough, the shape of breakthrough curves changed with iron contents as well (Figure 21). Under EBCT of 600 second, the slope of breakthrough curves became smaller with increase of iron content, which implies that arsenic intraparticle diffusion rate reduced with increase of iron content. This agrees with the finding in isotherm tests that longer equilibrium time is necessary for Fe-GACs.

REFERENCES

(1) Smedley, P. L.; Kinniburgh, D. G. A review of the source, behaviour and distribution of arsenic in natural waters. *Appl.Geochem.* **2002**, *17*, 517-568.

(2) Jain, C.; Ali, I. Arsenic: occurrence, toxicity and speciation techniques. *Water Res.* **2000**, *34*, 4304-4312.

(3) *Arsenic in drinking water*. National Research Council (NRC). National academy of sciences, Washington, DC, 1999.

(4) *Federal Register*. *66* (14), 6976-7066 . USEPA. 2001.

(5) Huang, C.; Vane, L. Enhancing As^{5+} removal by Fe^{2+} treated activated carbon. *J. water pollut. control fed.* **1989**, *61* (9), 1596-1603.

(6) Gu, Z.; Fang, J.; Deng, B. Preparation and evaluation of GAC-based iron-containing adsorbents for arsenic removal. *Environ. Sci. Technol.* **2005**, *39* (10), 3833-3843

(7) Vaughan, R. J.; Reed, B. Modeling As(V) removal by a iron oxide impregnated activated carbon using the surface complexation approach. *Water Res.* **2005**, *6* (39), 1005-1014.

(8) Chen, W.; Parette, R.; Zou, J.; Cannon, F. Arsenic removal by iron-modified activated carbon. *Water Res.* **2007**, *41*, 1851-1858.

(9) Mondal, P.; Balomajumder, C.; Mohanty, B. A laboratory study for the treatment of arsenic, iron, and manganese bearing ground water using Fe^{3+} impregnated activated carbon: Effects of shaking time, pH and temperature. *J. Hazard. Mater.* **2007**, *144* (1-2), 420-426.

(10) Fierro, V.; Muñiz, G.; Gonzalez-Sánchez, G.; Ballinas, M.L.; Celzard A. Arsenic removal by iron-doped activated carbons prepared by ferric chloride forced hydrolysis. *J. Hazard. Mater.* **2009**, *168*(1), 430-437.

(11) Muniz, G.; Fierro, V.; Celzard, A.; Furdin, G.; Gonzalez-Sánchez, G.; Ballinas, M.L. Synthesis, characterization and performance in arsenic removal of iron-doped activated carbons prepared by impregnation with Fe(III) and Fe(II). *J. Hazard. Mater.* **2009**, *165*, 893-902.

(12) Chang, Q.G.; Lin, W.; Ying, W.C. Preparation of iron-impregnated granular activated carbon for arsenic removal from drinking water. *J. Hazard. Mater*. **2010**, *184*, 515-522.

(13) Zhang, W.; Chang, Q.G.; Liu, W.D.; Li, B.J.; Jiang, W.X.; Fu, L.J. Selecting activated carbon for water and wastewater treatability studies. *Environ. Prog.* **2007**, *26*, 289-298.

(14) Hristovski, K.D.; Westerhoff, P.K.; Moller, T.; Sylverster, P. Effect of synthesis conditions on nano-iron (hydro)oxide impregnated granular activated carbon. *Chem. Eng. J.* **2009**, *146*(2): 237-243.

(15) Reed, B.; Vaughan, R. As(III), As(V), Hg, and Pb removal by Fe-oxide impregnated activated carbon. *J. Environ. Eng.* **2000**, *126* (9), 869-873.

(16) Zhang, Q.; Lin, Y.; Chen, X.; Gao, N. A method for preparing ferric activated carbon composites adsorbents to remove arsenic from drinking water. *J.Hazard. Mater.* **2007**, *148*, 671-678.

(17) Zhu, H.J.; Jia, Y.F.; Xu, X.; Wang, H. Removal of arsenic from water by supported nano zero-valent iron on activated carbon. *J. Hazard. Mater.* **2009**, 172, 1591-1596.

(18) Weber, W.J.Jr. *Physicochemical Processes for Water Quality Control*; Wiley-Interscience. 1972.

(19) Cooney, D.O. *Adsorption Design for Wastewater Treatment*; Lewis Publishers: New York, 1999.

(20) Zhang, S.J.; Li, X.Y.; Chen, J.P. Preparation and evaluation of a magnetite-doped activated carbon fiber for enhanced arsenic removal. *Carbon.* **2010**, 48, 60-67.
(21) *Second five-year review report for arsenic trioxide superfund site southeastern North Dakota*. USEPA. 2003.
(22) Jang, M.; Chen, W.F.; Cannon, F.S. Preloading hydrous ferric oxide into granular activated carbon for arsenic removal. *Environ. Sci. Technol*. **2008**, *42*(9), 3369-3374.
(23) Xu, C.; Teja, A. Supercritical water synthesis and deposition of iron oxide (α-Fe_2O_3) nanoparticles in activated carbon. *J. Supercritical Fluids* **2006**, *39*, 135–141.
(24) Liu, J. Comparative study on determination of iron contents in activated carbon. Linchan Huaxue Yu Gongye **1995**, 15, 57-61.
(25) Meng, X.G.; Bang, S.; Johnson, M.D.; Korfiatis, G.P. Chemical reactions between arsenic and zero-valent ironin water. *Abstr. Pap. Am. Chem. Soc.* **2002**, 224, 052-ENVR.
(26) Badruzzaman, M.; Westerhoff, P.; Knappe, D.R. Intraparticle diffusion and adsorption of arsenate onto granular ferric hydroxide (GFH). *Water Res*. **2004**, *38* (18), 4002-4012.
(27) *Trace elements in water, solids, and biosolids by stabilized temperature graphite furnace atomic absorption spectrometry.* USEPA. EPA-821-R-01-011. 2001.
(28) Thirunavukkarasu, O.; Viraraghavan, T.,; Subrama, K. Arsenic removal from drinking water using iron oxide-coated sand. Water Air Soil Pollut. **2003**, 142, 95-1114.
(29) Payne, K.; Abdel-Fattah, T. Adsorption of arsenate and arsenite by iron-treated activated carbon and zeolites: Effects of pH, temperature, and ionic strength. *J. Environ. Sci.Health A.* **2005**, *40* (4), 723-749.
(30) Weber, W.J.Jr.; Francis, A.D. *Process Dynamics in Environmental Systems*; John Wiley and Sons, Inc.: New York, 1996.
(31) Dzombak, D.A.; Morel, F.M.M. Surface Complexation Modeling: Hydrous Ferric Oxide; Wiley: New York. 1990.
(32) Faust, S.D.; Aly, O.M. *Adsorption Processes for Water Treatment*; Butterworths: London, 1987.
(33) Deliyanni, E.A.; Bakoyannakis, D.N.; Zouboulis, A.I.; Matis, K.A. Sorption of As(V) ions by akaganeite-type nanocrystals. *Chemosphere* **2003**, *50*,155-163.
(34) Chang, Q.G.; Lin, W. Development of GAC-Iron adsorbent for arsenic removal. Proc. of 82nd WEFTEC, Orlando, Florida, U.S.A. **2009**, 1552-1571.
(35) Myers, Drew. *Surfaces, interfaces, and colloids*; Wiley-VCH, 1999.
(36) Somorjai, G. *Introduction to Surface Chemistry and Catalysts*; John Wiley and Sons, Inc., New York, 1994.
(37) Benjamin, M.M. *Water Chemistry*; McGraw-Hill, 2002.
(38) Buche, B.; Owens, L. Removal of arsenic from ground water using granular activated carbon. *J. Am. Water Works Assoc.* **1996.**
(39) Chuang, C.L.; Fan, M.; Xu, M.; Brown,R.C.; Sung, S.; Saha, B.; Huang, C.P. Adsorption of arsenic(V) by activated carbon prepared from oat hulls. *Chemosphere* **2005**, *61*(4), 478-483.
(40) Budinova, T.; Petrov, N.; Razvigorova, M.; Parra, J.; Galiatsatou, P. Removal of Arsenic (III) from aqueous solution by activated carbons prepared from solvent extracted olive pulp and olive stones. *Ind. Eng. Chem. Res.*, **2006**, *45*, 1896-1901.
(41) Yang, L.; Wu, S.N.; Chen, J.P. Modification of acitvated carbon by polyaniline for enhanced adsorption of aqueous arsenate. *Ind. Eng. Chem. Res*. **2007**, *46*, 2133-2140.

(42) Ghanizadeh, G.; Ehrampoush, M.H.; Ghaneian, M.T. Application of Iron impregnated activated carbon for removal of arsenic from water. *Iranian J. Environ. Health Sci. Eng*. **2010**, *7*(2),145-156.
(43) Pierce, M. L.; Moore, C.B. Adsorption of arsenite and arsenate on amorphous iron hydroxide. *Water Res.* **1982,** *16*(7), 247-1253.
(44) Manning, B. A.; Hunt, M.; Amrhein, C.; Yarmoff, J. A. Arsenic(III) and arsenic(V) reactions with zerovalent iron corrosion products. *Environ. Sci. Technol.* **2002**, *36*, 5455-5461.
(45) Dixit, S.; Hering, J.G. Comparison of Arsenic(V) and Arsenic(III) Sorption onto Iron Oxide Minerals: Implications for Arsenic Mobility. *Environ. Sci. Technol.* **2003**, *37*(18), 4182-4189.